FINAL TECHNICAL REPORT

DE-SC0002217 **Lawrence R. Sita**

Investigation of Energy-Efficient Dinitrogen Activation and N-atom Transfer Processes

Postdoc: Dr. Jonathan Reeds (Ph.D. University of York, 2010)
Students: Brendan Yonke, Andrew Keane, Wesley Farrell
Contacts: University of Maryland, Rm 0300, Bldg 091, College Park, MD 20742
lsita@umd.edu

Project Timeframe: 09/01/2009 – 08/31/2012

Goals

The central hypothesis of the research program is that the unique steric and electronic features of the monocyclopentadienyl (η^5-C_5R_5), monoamidinate {η^2-[N(R^1)C(X)N(R^2)]} (CpAm) and guanidinate {η^2-[N(R^1)C(X)N(R^2)]} (CpGu) ligand environments are ideally suited for experimentally and computationally investigating groups 4, 5, and 6 early-transition-metal-mediated N_2 activation, N≡N bond cleavage, and N-atom functionalization within several isostructural series of CpAm- and CpGu-based dinuclear $[L_nM]_2(\mu$-$N_2)$ complexes in which the nature of the metal center can be varied as a function of group and row position, formal oxidation state and d^n electron count. Substantial advances made during the current year of funding provide strong justification and support for expanding the original goals of the research program to include the development of early-transition-metal catalysts that can utilize cheap and inexpensive nitrous oxide, N_2O, and carbon dioxide (CO_2) as 'green' chemical oxidants for the on-demand production of commodity chemicals, such as (1) the oxidative conversion of isocyanides to isocyanates according to: $N_2O + CNR \rightarrow N_2 + OCNR$ and (2) the deoxygenation of CO_2 and oxo transfer to substrate according to: $CO_2 + [S] \rightarrow CO + [S]O$. Finally, a third new focus area is the oxidation of CO according to: $N_2O + CO \rightarrow N_2 + CO_2$.

The specific aims of the project are to pursue a combined experimental and theoretical approach to: (1) establish energy profiles for all pathways leading to N_2, N_2O and CO_2 multiple bond activation and cleavage – including the molecular and electronic structures of ground-state precursors, intermediates and products, as well as those of interconnecting transition states, (2) determine relative energies and barrier heights for all structures and processes as a function of metal group and row position, formal metal oxidation state, d^n electron count, and (3) elucidate possible roles played by one- and two-electron reduced or oxidized species in facilitating these activation, multiple bond cleavage, and group transfer processes.

DOE Interest

The research goals of the present program seek to develop well-defined transition-metal-based homogeneous and solid-supported catalysts that can potentially serve to dramatically decrease the energy requirements, environmental impact and chemical safety concerns associated with the global production of commodity-scale chemicals. Fundamental knowledge gained from these studies include an elucidation of the factors that control the activation, multiple bond cleavage, and group transfer reactions of N_2, N_2O, CO_2 and N_3R, as well as, the mapping of mechanistic pathways and potential energy surfaces that lead to useful products under conditions that can provide significant energy savings and a decreased environmental impact.

I. Specific Aims. The central hypothesis of the research program is that the unique steric and electronic features of the cyclopentadienyl, amidinate (CPAM) and cyclopentadienyl, guanidinate (CPGU) ligand environments within groups 4 – 6 metal complexes, as depicted in Scheme 1, are ideally suited for experimentally investigating the coordination and 'fixation' of small molecules possessing X-Y multiple bonds (e.g., N_2, O_2, N_2O, CO and CO_2) in such a fashion that leads to (1) X-Y multiple bond cleavage through compensating formation of strong M-X and M-Y bonding interactions, and (2) pathways for atom-economical X- and Y-transfers to a substrate that serve to complete a catalytic cycle with respect to the starting CPAM or CPGU metal complex. An additional hypothesis is that these same features can be systematically manipulated and optimized across the entire early transition metal series of the periodic table to produce several families of *isostructurally-related* derivatives that differ only with respect to the nature of the metal center. If experimentally realized, it should then be possible to rapidly generate critically important structure/property/reactivity databases that provide both the motivation and support for theoretical (computational) and additional experimental investigations to establish key relationships between a metal's group and row position, formal oxidation state and d^n electron count, and relevant potential energy surfaces for metal-mediated activation of strong X-Y multiple bonds and subsequent X- and Y-atom and group transfers.

Scheme 1

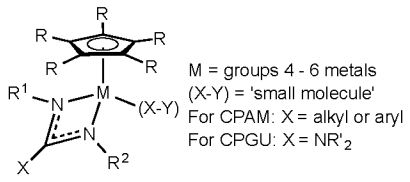

In support of these hypotheses, and in consideration of the body of preliminary results to be discussed, the following specific aims will be pursued:

1. Synthesis and characterization of *mid-valent* second- and third-row CPAM and CPGU group 5 (Nb, Ta) and group 6 (Mo, W) metal complexes that can serve as stable and readily available starting reagents for activating X-Y multiple bonds of small molecule substrates through metal coordination within molecularly-discrete complexes that are fully characterized both in solution using NMR, EPR, UV, IR spectroscopies, electrospray mass spectroscopy (ESMS), and electrochemistry, and in the solid state via single-crystal X-ray analysis, elemental analyses, IR and EPR spectroscopies.
2. Synthesis and characterization of molecularly discrete, mononuclear CPAM and CPGU $[M(XY)]_n$ (n = 1 or 2) metal complexes engaged in either strong X-Y multiple bond activation or post X-Y multiple bond cleavage, including terminal oxo, imido and nitrido complexes, $[L_nM(E)]$, where E = O, NR and N, respectively.
3. Documentation and investigation of stoichiometric oxygen atom transfer (OAT), sulfur atom transfer (SAT) and nitrene group transfer (NGT) processes involving CPAM and CPGU $[L_nM(E)]$ complexes and small molecule substrates of industrial relevancy.
4. Iterative optimization of steric and electronic features of precursors and intermediates for small molecule activation and atom- and group-transfer processes leading to release of value-added products of industrial interest within catalytically competent cycles that proceed with high chemical and energy efficiency.

Results

A. Synthesis and Characterization of CPAM and CPGU [$L_nM(XY)$] Complexes. To date, we have been successful in preparing and structurally characterizing several different families of isostructurally-related CPAM and CPGU group 4 – 6 metal complexes that can serve as precursors to different classes of corresponding [$L_nM(XY)$] complexes originating with the coordination of small molecule XY substrates. Most notable of these results are:

(i) Dinuclear bridging dinitrogen complexes, $\{(\eta^5\text{-}C_5Me_5)M[N(^iPr)C(R)N(^iPr)]\}_2(\mu\text{-}N_2)$ (M = Ti, Zr, Hf, V, Nb, Ta, Mo, W) (R = Me, Ph or NMe_2) (**1** – **8**). As Scheme 2 and Table 1 reveal, except for M = Cr, we have been able to prepare the entire family of group 4 – 6 dinuclear dinitrogen complexes supported by the common CPAM ligand set: $\eta^5\text{-}C_5Me_5$ (Cp*), $\eta^2\text{-}[N(^iPr)C(R)N(^iPr)]$. While not all of these derivatives were amenable to either isolation or crystallographic analysis, simple substitutions of the distal amidinate methyl group with either R = Ph or NMe_2 served to provide a complete series of crystallographically characterized derivatives. Complexes **1** – **8** were synthesized by chemical reduction

Scheme 2

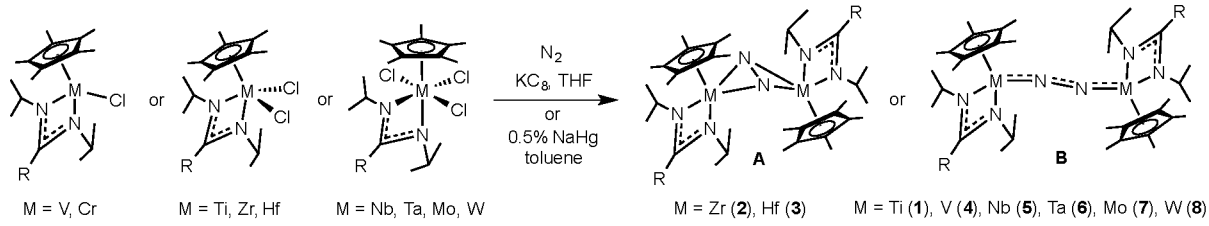

Table 1. *d*(NN) values obtained from single-crystal X-ray analyses of $\{Cp^*M[N(^iPr)C(R)N(^iPr)]\}_2(\mu\text{-}N_2)$.

M	Ti	Zr	Hf	V	Nb	Ta	Cr	Mo	W
A or B	A	B	B	A	A	A	--	A	A
d(NN) (Å)	1.270(2)	1.518(2)	1.611(4)	1.225(2)	1.300(3)	1.313(4)	--	1.267(2)	1.277(8)
R	Me	NMe_2	Me	Me	Ph	Me		Ph	Me
r_M (Å)[69]	1.60	1.75	1.75	1.53	1.64	1.70	1.39	1.54	1.62

of the corresponding metal chlorides of Scheme 2 using either potassium graphite (KC_8) in tetrahydrofuran (THF) from 77 K to room temperature (r.t.) or 0.5% sodium amalgam (NaHg) in toluene at r.t. Importantly, single crystal X-ray analyses of these dinuclear $\mu\text{-}N_2$ complexes provided the database of N-N bond distances, *d*(NN), shown in Table 1. Significantly, for M = Zr (**2**) and Hf (**3**) dinuclear coordination of the $\mu\text{-}N_2$ moiety occurs in 'side-on-bridging' ($\mu\text{-}\eta^2\text{:}\eta^2\text{-}N_2$) fashion (structure **A**), while for all the other metals, M = Ti, V, Nb, Ta, Mo and W, (**1** and **4** – **8**, respectively), an 'end-on-bridging' ($\mu\text{-}\eta^1\text{:}\eta^1\text{-}N_2$) motif (structure **B**) was established. Further, as Table 1 reveals, the *d*(NN) values for **2** and **3** are remarkably large vis-à-vis other known dinuclear dinitrogen complexes and for the related hafnium derivative, $\{Cp^*Hf[N(Et)C(Me)N(Et)]\}_2(\mu\text{-}\eta^2\text{:}\eta^2\text{-}N_2)$, *the d(NN) of 1.635(3) Å remains the largest value ever reported for the activation of N_2 through dinuclear complexation.* Finally, a comparison of the experimentally-derived covalent radii, r_M, of the early transition metals (see Table 1) provide possible clues regarding the preference of structure **A** vs **B** within the series and our inability (so far) to obtain an analogous chromium derivative.[69] More specifically, Zr and Hf have the largest r_M value at 1.75 Å, which might be required to accommodate dinuclear side-on-bridging $\mu\text{-}N_2$ coordination. The next largest metal covalent radius is Ta at 1.70 Å, and this value might represent the breakpoint at which a linear dinuclear end-on-bridging $\mu\text{-}N_2$ motif is now established as the lowest energy structure (vide infra). This geometry then remains the observed coordination mode for the remaining metals that have r_M values of < 1.65 Å. Finally, the substantially smaller r_M of 1.39 Å for Cr is quite conceivably unable to support dinuclear coordination of N_2 in either **A** or **B** fashion, at least with the CPAM and CPGU derivatives that have been investigated to date.

(ii) N-N Bond Cleavage in {Cp*M[N(^{i}Pr)C(R)N(^{i}Pr)]}$_2$(μ-N_2) Derivatives. Access to an entire early transition metal series of isostructurally-related CPAM / CPGU dinuclear μ-N_2 derivatives provides a unique opportunity to investigate and establish what role steric (ligand) and electronic (metal) factors might play in controlling the barrier height of potential N-N bond cleaving reaction pathways involving these complexes. In this regard, although displaying large *d*(NN) values, which can be taken as an indicator of a high degree of N≡N bond 'activation', the second- and third-row group 4 metal derivatives, **2** and **3**, are thermally and photolytically robust in solution. This is not an unexpected observation given the formal [M(IV, d^0), M(IV, d^0)] oxidation states assigned to the metal centers in these dinuclear μ-N_2 complexes – that is to say, the group 4 metals simply do not possess the total number of reducing d^n electrons required for complete N-N bond cleavage (i.e., 6 electrons total). On the other hand, and in spite of much smaller *d*(NN) values, the second- and third-row group 5 analogues, **5**, **6** and **9-11**, all undergo quantitative thermal N-N bond cleavage in solution to provide the corresponding dinuclear bis(μ-nitrido) products, {Cp*M[N(^{i}Pr)C(R)N(^{i}Pr)(μ-N)}$_2$ (M = Nb and Ta) (**12 - 16**, respectively), according to Scheme 3. In addition, we have been able to demonstrate the ability to tune the energy barrier for this thermal N-N bond cleavage process through subtle manipulation of non-bonded steric interactions within

Scheme 3

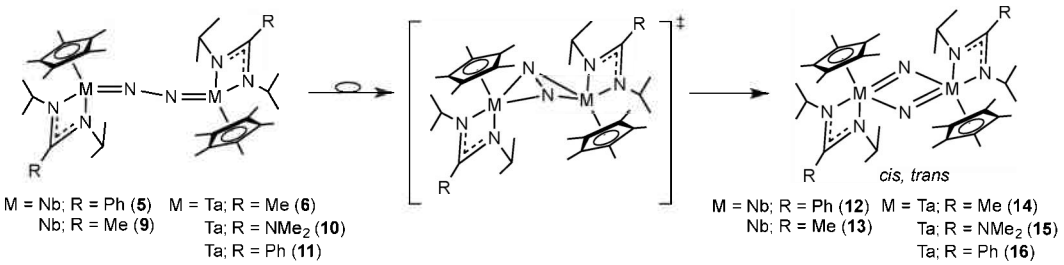

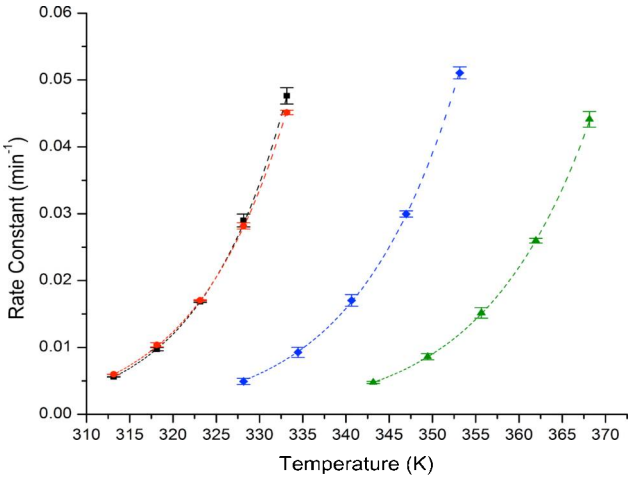

Figure 1. Temperature dependent rate constants fitted to the Eyring equation for the conversion of (black) **6→14**, (blue) **10→15**, (green) **11→16** and (red) **5→12**,

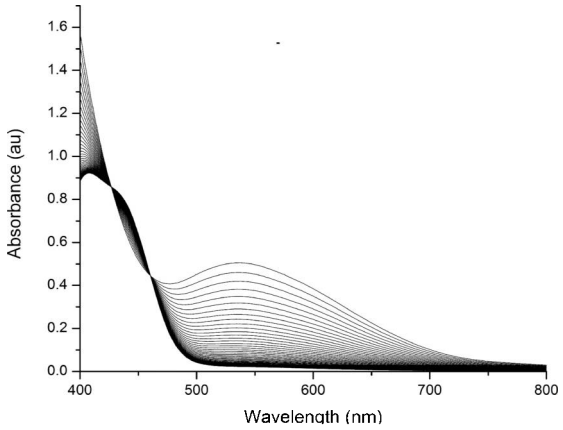

Figure 2. UV-Vis scanning kinetics at λ 625 nm [T = 318.15 K, Δt = 9 min, (t_f – t_o) = 300 min] for thermal conversion of **6→14**.

the

Table 2. Experimental activation parameters for thermal conversion of group 5 dinuclear μ-N_2 complexes.

	$\Delta G^{\ddagger}$ (kcal/mol)[a,b]	$\Delta H^{\ddagger}$ (kcal/mol)[b]	$\Delta S^{\ddagger}$ (cal/mol-K)[b]
6 → 14	24.3(3)	21.5(3)	-8.4(9)
10 → 15	25.5(3)	20.6(3)	-14.6(8)
11 → 16	26.6(3)	21.7(3)	-14.4(8)
5 → 13	24.4(1)	20.2(1)	-12.4(5)

[a]Calculated at T = 338.15. [b]Error reported at the 95% confidence interval

ligand environment by simply changing the nature of the distal group where R = Me, Ph and NMe_2. Based on the results of extensive structural and kinetic investigations shown in Figure 1, we propose that thermal N-N bond cleavage in these group 5 derivatives proceeds through an intramolecular μ-η^1:η^1-N_2 → μ-η^2:η^2-N_2 rearrangement in which the magnitude of steric interactions within the side-bound μ-N_2 intermediate or transition state can now be seen to establish the barrier height for the rate-determining step that has an associated negative $\Delta S^{\ddagger}$ value as presented in Table 2. Originally proposed by us,[58] this mechanism has now been validated on theoretical grounds through a detailed computational study by Musaev and co-workers.

To the best of our knowledge, our experimental results obtained for the second- and third-row group 5 dinuclear μ-N_2 complexes represent the first ever demonstration of the ability to modulate the energy barrier height of a N-N bond cleaving process related to the activation and fixation of molecular N_2 – and this includes all past investigations of solution-phase transition metal chemistry, the heterogeneous Haber-Bosch process and the chemical biology of nitrogenase enzymes.

In contrast to Nb and Ta, the first-row vanadium analogue, **4** (see Scheme 2), proved to be thermally robust in solution, and once again, we speculate that this stability might originate, in large part, to a smaller metal covalent radius of the first-row vis-à-vis the second- and third-row metals (*cf.* 1.53 Å vs. 1.64, 1.70 Å, respectively, see Table 1). The observed thermal solution stability of the second- and third-row group 6 derivatives, **17** and **8** (R = Me), might then be accounted for in similar fashion. Surprisingly, however, in unpublished results, both of these compounds were found to undergo clean photoconversion (medium-pressure Hg lamp) in solution to the corresponding group 6 dinuclear bis(μ-nitrido) complexes **18** and **19** that possess an unprecedented formal [M(V, d^1), M(V, d^1)](μ-N)$_2$ electronic configuration as shown in Scheme 4. In order to confirm the structural identity of these two new photochemical products, an alternative synthetic route was developed that proceeds by reaction of the corresponding M(IV) dichlorides, **20** and **21**, with an excess of trimethylsilylazide (TMSA) to generate the M(VI) terminal nitrido, chloride intermediates, **22** and **23**, respectively, which were then subsequently reduced with 0.5% NaHg to provide excellent yields of the dinuclear bis(μ-N) complexes according to Scheme 4.

Scheme 4

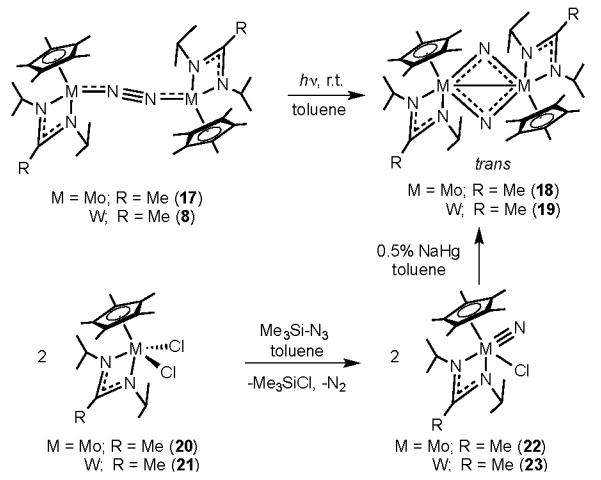

(iii) Group 6 Dinuclear μ-N_2 Complexes as M(II) Synthons. In keeping with the formal oxidation state suggested by solid-state molecular structures, the group 6 dinuclear μ-N_2 complexes **7**, **17** for M = Mo and **8** for M = W, have proven to be highly versatile M(II) synthons for generating a wide variety of new CPAM group 6 metal complexes arising from either simple displacement of N_2 through coordination (activation) of multiply-bonded X-Y substrates that can serve as better π-acceptor ligands, or through complete X-Y multiple-bond cleavage. Table 3 presents a library of some of the more intriguing

Table 3. Products from reaction of group 6 dinuclear μ-N_2 complexes with small molecule X-Y substrates.

	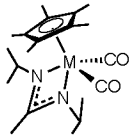		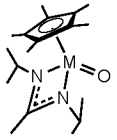		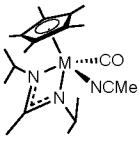	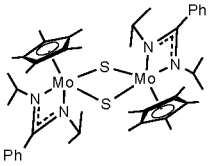
M =	Mo (**24**) W (**25**)	Mo (**26**) W (**27**)	Mo (**28**) W (**29**)	Mo (**30**) W (**31**)	Mo (**32**)	Mo (**33**)
X-Y	CO	CNR	N_2O, CO_2	N_3R	CO, NCMe	S_8, S=CNR

structurally-characterized products that have been isolated to date, and in all cases, the formal oxidation state of the metal center can be described as being either M(II) (**24** – **27**) or M(IV) (**28** – **33**). Fortunately, the vast majority of the CPAM and CPGU group 5 and 6 metal complexes have been amenable to structural characterization by single-crystal X-ray analyses, which has proven critical for establishing the identity of the multitude of open-shell (d^1, d^3) or high-spin (d^2) mid-valent complexes that we have worked with. Table 4 presents a small sampling of the large database of molecular structures that have been obtained for these and several other unique classes of compounds to be discussed.

Table 4. Molecular structures of CPAM group 6 metal complexes arising from small molecule activation.

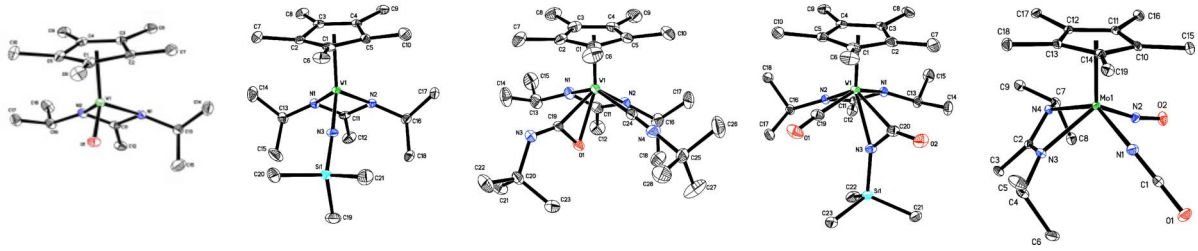

(iv) Catalytic Oxygen Atom Transfer (OAT), Nitrene Group Tranfer (NGT) and Sulfur Atom Transfer (SAT). We have been very successful in developing a rich chemistry surrounding the complexes shown in Tables 3 and 4 as precursors and intermediates within a variety of catalytic metal-mediated atom- and group-transfer processes involving small molecules fixation. As Scheme 5 presents, the most significant of these results has been the development of *catalytic orthogonal routes to isocyanates based on a common CPAM group 6 metal complex platform* and that proceed under nearly ambient temperatures and pressures by either OAT according to: N_2O + CNR → N_2 + OCNR (cycle a) or NGT according to: N_3R + CO → N_2 + OCNR (cycle b). Importantly, the proposed mechanisms shown are supported by a wealth of molecular structures (see Tables 3 and 4) and spectroscopic data e.g., NMR, IR, UV-Vis) for all key intermediates that have been separately isolated and fully characterized in solution through extensive use of isotopically-labeled substrates (e.g. ^{13}CO, $^{13}CO_2$, $^{15}N_2$, and $^{15}N_2O$). As a further example of the latter, Figure 3 presents the results of a time-dependent ^{13}C NMR spectroscopic study of the degenerative OAT between labeled-^{13}CO and CO_2 that is catalyzed by the CPAM group 6 terminal oxo complex **28** through the mechanism presented in Scheme 6.

Scheme 5

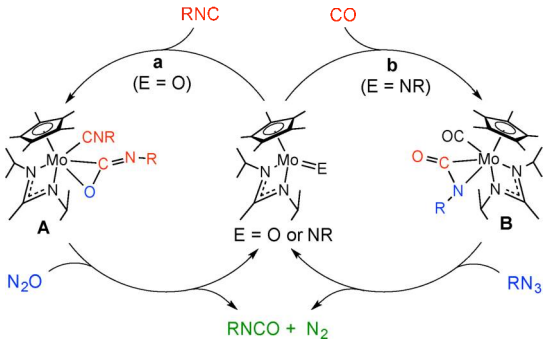

Scheme 6

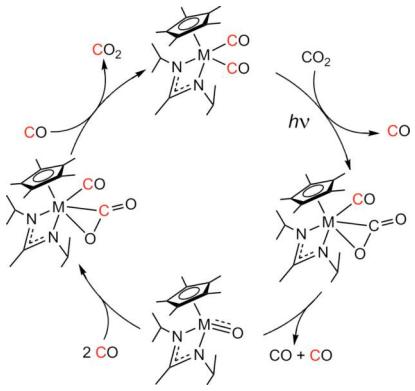

To the best of our knowledge, the ability of a group 6 M(II) / M(IV) catalytic cycle for both OAT and NGT that proceeds under near ambient conditions is unprecedented.

During the course of investigations to establish the identities and reaction pathways presented in Schemes 5 and 6, several additional path-breaking results have been established, some of which are presented in Scheme 7. For instance, when CNR is replaced by CO in catalytic cycle a on the left-hand side of Scheme

5, an excellent 80% yield of the product arising from CO-mediated N-N bond cleavage of N_2O, **34**, was obtained. Observation of N-N bond cleavage that is competitive with OAT from N_2O to form a metal oxo is extremely rare, and recently, Wang et. al. performed an extensive theoretical (computational) investigation which validated, with minor revision, our proposed mechanism shown in Scheme 7. We have further designed and synthesized the structurally-characterized monocarbonyl, acetonitrile complex, **32** (see Table 3) as a useful mechanistic probe that can substitute for a coordinatively unsaturated monocarbonyl intermediate that is generated through photolytic dissociation of CO. according to Scheme 7. More importantly, reaction of X-Y small molecules with **32** can provide an alternative 'dark path' entry into the same photolytically-driven catalytic cycles. We have also discovered that **32** can provide access to several new, and unexpected, products arising from X-Y coordination and X-Y bond cleavage. For instance, as Scheme 8 reveals, reaction of elemental sulfur, S8, with the dinuclear (μ-N_2) complex **5** (R = Ph), provides an excellent yield of the [Mo(IV), Mo(IV)] bis(μ-sulfido) complex **33** as a mixture of cis and trans isomers. Reaction of **32** with S_8, on the other hand, produces an excellent yield of the Mo(IV)(CO)(η^2-S_2) complex **35**, which can then be converted into the isomeric dithiocarbonate, Mo(IV)[κ^2-(S,S)-S_2CO] **36** (see Scheme 8). Conversion of **35** to **36** suggested a possible mechanism involving elimination of carbonylsulfide, O=C=S, to generate a transient mononuclear Mo(IV) terminal sulfido that is then trapped by re-addition of COS to the more thermodynamically favored product. In analogy then to the catalytic cycles of Schemes 5 and 6, we hypothesized that a similar catalytic cycle mediated by 24 (R = Ph) under photolyic conditions could be developed that proceeds via: CO + S_n → COS + S_{n-1}. Gratifyingly, as the ^{13}C NMR data presented in Figure 4 attest, substantial progress towards achieving this goal has been made with the desired transformation so far proceeding in stoichiometric fashion with concomitant formation of **36** as the thermodynamic sink according to Scheme 9. At the present time, we also cannot account for the unbalanced stoichiometry with respect to Mo.

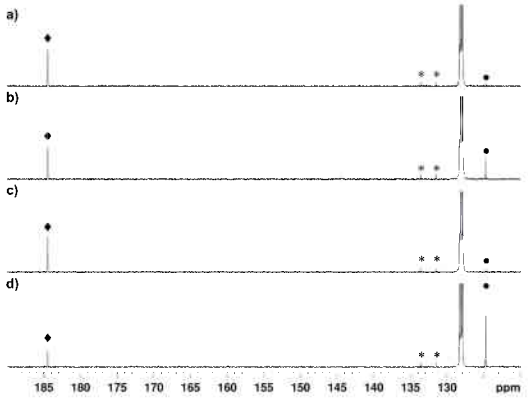

Figure 3. ^{13}C NMR spectra taken at timed intervals for the degenerative OAT between ^{13}CO (185 ppm) and CO_2 (125 ppm)

Scheme 7

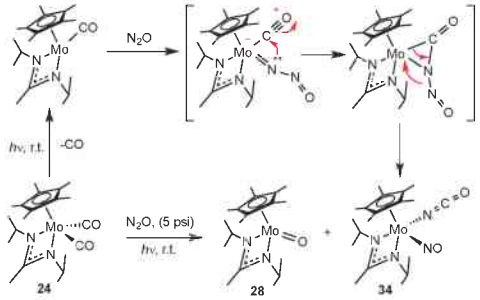

Scheme 8

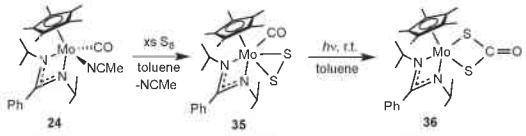

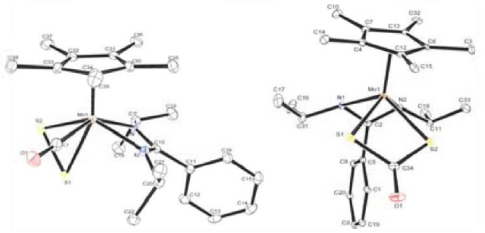

However, to the best of our knowledge, the present results represent the first observation of metal-mediated oxidation of CO by elemental sulfur that proceeds at near ambient conditions.

We have also been successful in developing a closely related catalytic oxidation of isonitriles to thioisocyanates that proceeds through the proposed catalytic cycle of Scheme 10 according to: CNR + S_n → SCNR + S_{n-1}. We believe that the key to successful turnover for this catalytic process lies with the fact

Scheme 9

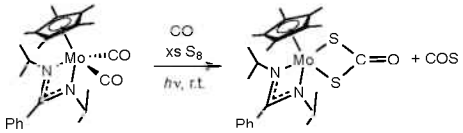

Scheme 10

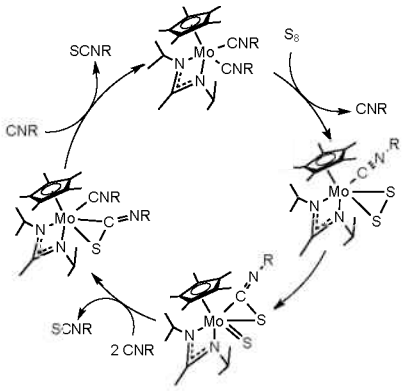

that the Mo(II) bis(CNR) complex **26** readily loses the more weakly coordinated isonitrile ligands that allows the catalytic oxidation to proceed in the dark.

(v) Towards development of a 'Schrock cycle' for N_2-fixation. In 2003, Yandulov and Schrock successfully realized the goal of catalytic N_2 fixation to ammonia, NH_3, using the triamidoamine Mo(III, d^3) dinitrogen complex, $[(ArNCH_2CH_2)_3N]Mo(\kappa^1\text{-}N_2)$ [Ar = 3,5-(2,4,6-iPr_3-C_6H_2)$_2$$C_6H_3$] in conjunction with multiple equivalents of reagents to deliver the required number of electrons and protons to reduce coordinated N_2 to two equivalents of free NH_3 within a non-aqueous solvent (heptane). As presented in Chart 1, the key N-N bond-cleaving steps, of what is now commonly referred to as the 'Schrock cycle', proceed through protonation of a Mo(V, d_1) hydrazido intermediate (II) to generate the corresponding Mo(V) hydrazidium species (III), which, upon one-electron reduction, disproportions to produce a Mo(VI, d_0) nitride (IV) and one equivalent of NH_3. Protonation of IV yields the cationic parent imide V that is then converted back to I through additional electron and proton additions under an N2 atmosphere to complete the catalytic cycle (not shown). Recently, we documented an analogous series of mid-valent CPGU group 5 Ta(IV, d^1) hydrazido and hydrazidium complexes, the latter of which engages in one-electron reduction and facile N-N bond cleavage chemistry with generation of a Ta(V, d^0) nitride and cationic Ta(V, d^0) parent imide according to Eq. (b) of Chart 1 and Scheme 11. Isolation of cis, trans-**14** through chemical reduction of the Ta(IV) hydrazidium is consistent with transient generation of the terminal Ta(V) nitrido species **37** followed by dimerization according to Scheme 11. While mechanistic origins of the structurally-characterized parent imide product **38** are less clear, we speculate that a slower rate of

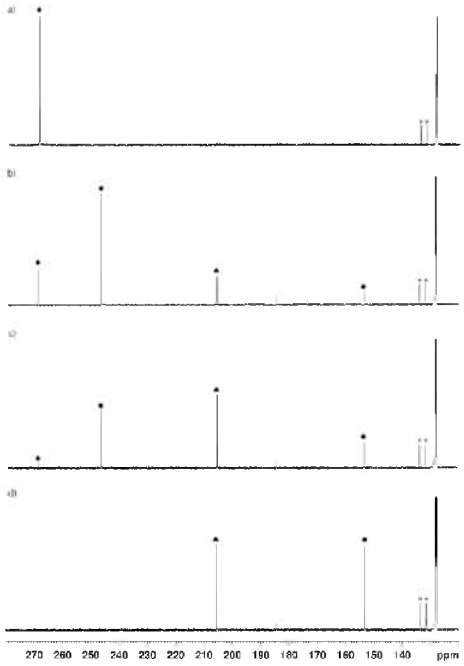

Figure 4. ^{13}C NMR spectra taken at timed intervals for the oxidation of unlabeled CO to ^{13}COS (circle) with S_8 as mediated by Mo(^{13}CO)$_2$ **24** (R = Ph) (diamond) and with concomitant formation of first **35** (triangle) and ultimately **36** (triangle). Internal standard (durene) is marked with asterisk

Chart 1

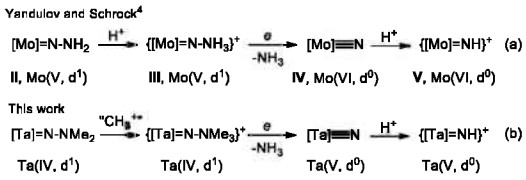

Scheme 11

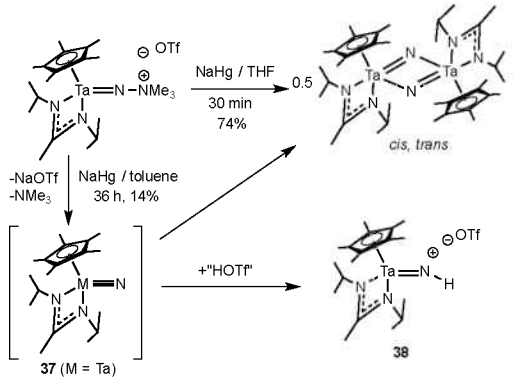

reduction in toluene leads to a lower solution concentration of **37** and thereby, providing the opportunity for other reaction pathways to compete with bimolecular dimerization, such as protonation of a Ta(V) imide anion with adventitious proton sources.

Publications from Work Performed.

[1] Fontaine, P. P.; Yonke, B. L.; Zavalij, P. Y.; Sita, L. R. "Dinitrogen Complexation and Extent of N≡N Activation within the Group 6 "End-On-Bridged" Dinuclear Complexes $\{(\eta^5\text{-}C_5Me_5)M\text{-}[N(iPr)C(Me)N(iPr)]\}_2(\mu\text{-}\eta^1\text{:}\eta^1\text{-}N_2)$ (M = Mo and W)," *J. Am. Chem. Soc.* **2010**, *132*, 12273-12285.

[2] Yonke, B. L.; Reeds, J. P.; Zavalij, P. Y.; Sita, L. R. "Catalytic Degenerate and Nondegenerate Oxygen Atom Transfers Employing N_2O and CO_2 and a M(II)/M(IV) Cycle Mediated by Group 6 M(IV) Terminal Oxo Complexes," *Angew. Chem. Int. Ed.* **2011**, *50*, 12342-12346.

[3] Reeds, J. P.; Yonke, B. L.; Zavalij, P. Y.; Sita, L. R. "Carbon Monoxide-Induced N-N Bond Cleavage of Nitrous Oxide That is Competitive with Oxygen Atom Transfer to Carbon Monoxide as Mediated by a Mo(II)/Mo(IV) Catalytic Cycle," *J. Am. Chem. Soc.* **2011**, *133*, 18602-18605.

[4] Yonke, B. L.; Keane, A. J.; Zavalij, P. Y.; Sita, L. R. "Mononuclear tantalum(IV, d^1) imido complexes supported by the monocyclopentadienyl, amidinate and guanidinate ligand sets as models to explore dinitrogen fixation by "end-on-bridged" dinuclear $\{[Ta(IV, d^1)]\}_2(\mu\text{-}\eta^1\text{:}\eta^1\text{-}N_2)$ complexes," *Organometallics* **2012**, *31*, 345-355.

[5] Keane, A. J.; Zavalij, P. Y.; Sita, L. R. "N-N Bond Cleavage of Mid-Valent Ta(IV) Hydrazido and Hydrazidium Complexes Relevant to the Schrock Cycle for Dinitrogen Fixation," *J. Am. Chem. Soc.* **2013**, *135*, 9580-9583.

[6] Keane, A. J.; Yonke, B. L.; Hirotsu, M.; Zavalij, P. Y.; Sita, L. R. "Fine-Tuning the Energy Barrier for Metal-Mediated Dinitrogen NN Bond Cleavage," *J. Am. Chem. Soc.* **2014**, *136*, 9906-9909.

[7] Yonke, B. L.; Reeds, J. R.; Fontaine, P. P.; Zavalij, P. Y.; Sita, L. R. "Catalytic Production of Isocyanates via Orthogonal Atom and Group Transfers Employing a Shared Formal Group 6 M(II)/M(IV) Redox Cycle," *Organometallics* **2014**, *33*, 3239-3242.

[8] Yonke, B. L.; Reeds, J. R.; Zavalij, P. Y.; Sita, L. R. "Atom- and Group Transfers to M(IV) Oxo and Imido Complexes, $(\eta_5\text{-}C_5Me_5)M[N(^i Pr)C(Me)N(^i Pr)](E)$ (M = Mo, W; E = O, $NSiMe_3$): Orthogonal Generation of a M(VI) Terminal Nitride via Inter-ligand Silyl Group Migration," *Zeit. Anorg. Alleg. Chem.* **2014**, in press.